Volume: 8 | Issue: 4 | 2024 | December

The influence of aluminum-doped ZnO films on multi-chip remote-phosphor white LEDs' properties

Hsin-Yi Ma [1], *Nguyen Doan Quoc Anh*[2,*]
[1]Department of Industrial Engineering and Management, Minghsin University of Science and Technology, Hsinchu, Taiwan.
[2] Faculty of Electrical and Electronic Engineering, Ton Duc Thang University, Ho Chi Minh City, Vietnam.

*Corresponding Author: Nguyen Doan Quoc Anh (email: nguyendoanquocanh@tdtu.edu.vn)
(Received: 09-July-2024; accepted: 07-November-2024; published: 31-December-2024)
http://dx.doi.org/10.55579/jaec.202484.467

Abstract. *Zinc oxide (ZnO) exhibits stable emission across blue, green, orange, and red wavelength regions, depending upon excitation energy and preparation conditions. It is possible to tune the ZnO luminescent bandgap by introducing metal dopants to generate extrinsic defects in its matrix. Leveraging this stable and tunable photo-luminescent characteristic, ZnO emerges as a promising candidate for luminescent materials, especially applicable in the realm of luminescent converted LEDs. Specifically, aluminum-doped ZnO (Al-doped ZnO) films exhibit commendable conductivity and transmittance, qualifying them as suitable candidates for transparent conducting oxide materials crucial in LEDs. This study presents a novel application of Al-doped ZnO films, synthesized through a cost-effective sol-gel method, as a converter layer in white LED technology. The research systematically explores the impact of varying Al-doped ZnO concentrations on the color properties and luminosity of the white LED, with the goal of identifying the optimal concentration to achieve enhanced LED lighting efficiency.*

Keywords: *Color uniformity, color rendering, luminous flux, optical scattering, white LED.*

1. Introduction

The escalating demand for light-emitting diodes (LEDs) and solid-state lighting systems underscores the transformative impact of this technology on various industries [1–3]. Particularly, LEDs designed for space lighting applications predominantly rely on blue-emitting GaN LEDs coupled with color-converting phosphors. Among these phosphors, the yellow-emission YAG:Ce^{3+} has emerged as a cornerstone, despite challenges related to low stability and thermal quenching [4–6]. To address these limitations, various blue light excitable yellow-emitting phosphors have been developed, such as Ce^{3+}-doped $LaSr_2AlO_5$ and Eu^{2+}-doped $Sr_3(Al_2O_5)Cl_2$, yet their implementation often results in low Color Rendering Index (CRI) lighting output due to the absence of red color emission. To enhance the CRI efficiency for the LED white light emission, researchers have explored the integration of blue light excitable red-emitting phosphors alongside green or yellow phosphors. However, achieving optimal LED efficiency necessitates meticulous control over particle size, weight, and synthesis techniques for multiple phosphors [7–9].

In this context, zinc oxide (ZnO) emerges as a promising semiconductor for optoelectronic applications, owing to its wide direct bandgap, high exciton binding energy, chemical and thermal stabilities, low cost, and environmental friendliness. Despite its advantageous properties, ZnO's wide bandgap limits its absorption in the visible light region, making it inefficiently excited under visible blue excitation sources. Researchers carried out many works and demonstrated that the ZnO nanowires showed enhanced visible-light absorption [10, 11]. Moreover, doping metals such as Al and Fe with ZnO nanowires allowed the compound to be excitable by UV and blue light, enlarging the application range of the ZnO material. Al-doped ZnO films, in particular, exhibit excellent conductivity and high transparency in the visible light range, making them suitable for transparent conducting oxide materials used for solar cells and LEDs [12]. The high transparency of the Al-doped ZnO film allows the emitted light to pass through the material without significant absorption or loss, which is essential for high-luminosity LED devices. The doping of ZnO with aluminum also enhances its n-type semiconducting properties, which is essential in LED structures to create the necessary junctions (p-n junctions) that enable light emission when current flows through the diode. Additionally, the Al-doped ZnO materials hold promise in the large-scale production of LED because of the abundance and low cost of the components Al and ZnO. Therefore, the Al-doped ZnO turns out to be the potential luminescent converter for the white LED package, in addition to the phosphor material. In this research, we present the utilization of Al-doped ZnO films prepared through a cost-effective sol-gel method as a converter layer in white LED technology. This study explores the impact of varying Al-doped ZnO concentrations on the color properties and luminosity of the prepared white LED, aiming to identify the optimal concentration for achieving superior LED lighting efficiency.

2. Experimental

The Al-doped ZnO compound was prepared using the sol-gel method, as demonstrated in the following steps [13–15].

- Zinc acetate was mixed with aluminum nitrate and a solution of urea in ethanol. The amounts of each component in the mixture are 0.85 mol, 0.15 mol, and 3 mol of zinc acetate, aluminum nitrate, and urea/ethanol solution, respectively.
- The mixed solution was stirred and evaporated for an hour at a temperature of about 70°C to obtain a transparent gel.
- The gel was put into a closed muffle furnace and burned for 3 hours at a temperature of 300 degrees Celsius.
- After heated, the obtained yellow mass was cooled down naturally to room temperature, followed by grinding in mortar to get the required Al-doped ZnO powder.

For the LED's configuration, we utilized the structure of remote phosphor deposition, since the remote phosphor structure can hinder the significant amount of photons absorbed by the LED chip by utilizing a sufficient distance between the converter film and the chips' surfaces [16]. As depicted in Fig. 1, the LED assembles the Al-doped ZnO film placed above a pack of nine blue chips. Particularly, the 3D simulation of the LED model is depicted in Fig. 1a using LighTools software, and the cluster of bonded chips for the LED is in Fig. 1b.

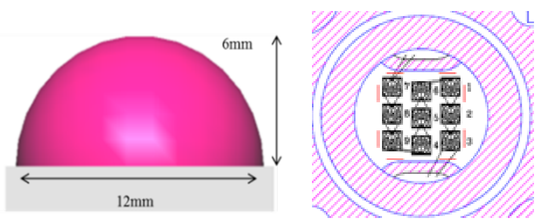

Fig. 1: The modeled LED: (a) the 3D simulation of the LED by LightTools software and (b) the chip wire-bonding map.

3. Results and discussion

The transmittance intensity of the LED with 0-50 wt% of Al-doped ZnO is displayed in Fig. 2. Generally, the transmittance band includes two regions, one is around 455 nm and the other is within 500-620 nm. The 455 nm is the band that originates from the blue-chip emission, and the 500-620 nm is mainly from the Al-doped ZnO compound. Besides, the second broad emission band (500-620nm) has the most intense peak centered at 570 nm, regardless of the Al-doped ZnO amounts. We also noticed another lower-intensity peak in this emission band centered at 540 nm, which could be attributed to the ZnO itself. The peak emission observed in the visible yellow-orange region is a consequential outcome of the luminescence-related defects. This phenomenon is presumed to originate from defects associated with the presence of oxygen vacancies (Vo) and interstitial oxygen (Oi), both created by the doping of Al^3+ in the Zn^2+ site. Nevertheless, increasing Al-doped ZnO results in the decrease of the mentioned emission peaks, probably owing to the optical scattering strength in the presence of the denser Al-doped ZnO film [17–19].

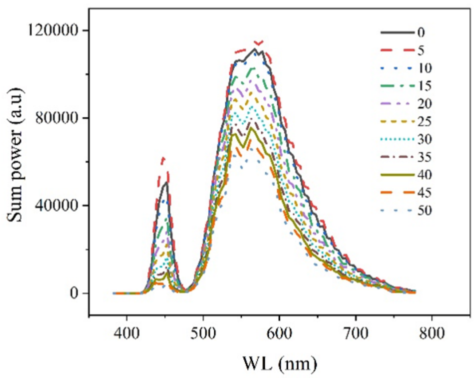

Fig. 2: Transmittance intensity of the white LED with altering the concentration of Al-doped ZnO.

The Al doping also changes the scattering factor of the ZnO matrix, meaning that varying the Al-doped ZnO amount impacts the scattering performance of the LED package. We used a Mie-scattering-based computational framework to compute the optical scattering within the phosphor film [20–22], specifically with varying concentrations of ZnO. The central aim was to ascertain the reduced scattering coefficient (δ_{sca}) of the phosphor layer, mathematically expressed through equations 1 and 2

The computation incorporates key parameters including the total distribution density of luminescent particles ($N(r)$), the wavelength of incident light (λ), particle radius (r), scattering coefficients ($\mu_{sca}(\lambda)$), and scattering cross-sections (C_{sca}).

$$\delta_{sca} = \mu_{sca}\left(1-g\right) \tag{1}$$

$$\mu_{sca}\left(\lambda\right) = \int N(r)C_{sca}\left(\lambda, r\right)dr \tag{2}$$

The obtained reduced scattering data are illustrated in Fig. 3. Initially, the small increase of ZnO concentration of 5-10 wt% does not impact much on the scattering factor as two scattering lines in the graph coincide. Further increasing the ZnO amount leads to higher values of the reduced scattering parameter. Besides, the longer wavelength presents a lower scattering strength, which can be demonstrated with Mie-scattering for spherical particles.

Less Al-doped ZnO amount will create more voids in the luminescent converting film, allowing the light to be transmitted easily, or higher light extraction can be obtained. In contrast, higher Al-doped ZnO concentration leads to a denser film or less transparent converting film, reducing the extraction of light while improving the optical scattering. Thus, the lower transmittance intensity of the LED was observed. This also resulted in the declining lumen output of the LED on the increasing Al-doped ZnO concentration, as seen in Fig. 4 (Al-doped ZnO is shortened as ZnO hereafter in the figures). However, compared to the un-deposited Al-doped ZnO package, the lumen output of 5wt% Al-doped ZnO sample is fairly higher, indicating that the Al-doped ZnO film contributes to yielding better luminosity for white LED lighting.

The introduction of Al-doped ZnO in the LED results in the generation of warm white light with a correlated color temperature (CCT) level of around 4000 K. Yet, when compared with the undoped package, the Al-doped ZnO doped LED has induced a modest expansion in the CCT range across diverse viewing angles. Remarkably, the resultant white light maintains its warmth, falling within the temperature range of 3900-4025 K, as portrayed in Fig. 5. Yet, it is essential to underscore the notable fluctuations observed in the angular CCT ranges concerning

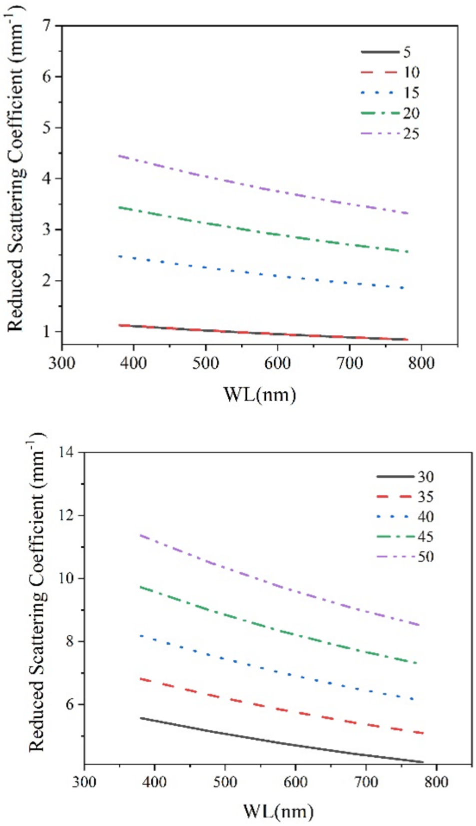

Fig. 3: Reduced scattering parameter with various concentrations of Al-doped ZnO.

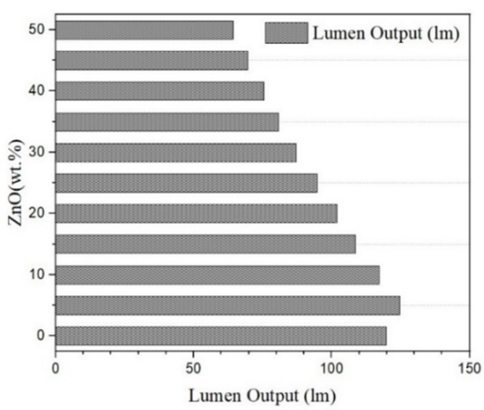

Fig. 4: Lumen output changes with altering concentration of Al-doped ZnO.

different Al-doped ZnO concentrations. Beyond 20 wt% of Al-doped ZnO in use, the CCT range is relatively stable, coinciding with a discernible reduction in intensity at the direct viewing angle (0^o). efficiency in reducing scattering. Intriguingly, the most stable-like reduction implies an enhanced dispersion of light towards the edges of the package, attributable to the heightened angular CCT range is affiliated with an Al-doped ZnO concentration of 45 wt%, showcasing the smallest CCT values between the largest ($\pm 60^o$) and the direct (0^o) viewing angles. Such results indicate that the increase in the percentage of Al-doped ZnO in the converter film induces the dispersion of light and wider scattering angles. As a result, better light distribution uniformity is achievable.

The pursuit of optimal color uniformity is integral to advancing high-quality white LED devices, where visual comfort for human eyes is the paramount consideration. The delta-CCT, as illustrated in Fig. 6, emerges as a crucial metric for quantifying color variation, and our research underscores the role of Al-doped ZnO film in supporting enhanced color dispersion through improved scattering properties. The attainment of the lowest delta-CCT, indicative of superior uniformity, is notably observed at an Al-doped ZnO concentration of 45 wt%, demonstrating a reduction of approximately 75 K compared to data of the undoped sample. Furthermore, Al-doped ZnO concentrations within the range of 20-25 wt% and even at 50 wt% exhibit lower delta-CCT values than those of the undoped sample. Conversely, a ZnO concentration of 15 wt% is associated with the highest delta-CCT, signifying a less uniform chromatic distribution. In summary, the ideal ZnO concentration for optimal color uniformity is identified as 45 wt% or, at the least, falls within the range of 20-25 wt%.

Moreover, the augmentation of blue light scattering and absorption with increasing Al-doped ZnO concentration plays a pivotal role in enhancing color reproduction by intensifying the conversion of blue light to the longer yellow-orange. Figures 7 and 8 showcase the comprehensive Color Quality Scale (CQS) and Color Rendering Index (CRI) performance across varying Al-doped ZnO concentrations [23–25]. Particularly noteworthy is the significant improvement observed at 5 wt% Al-doped ZnO, highlighting its capacity to enhance chroma reproduction in white LED light. This

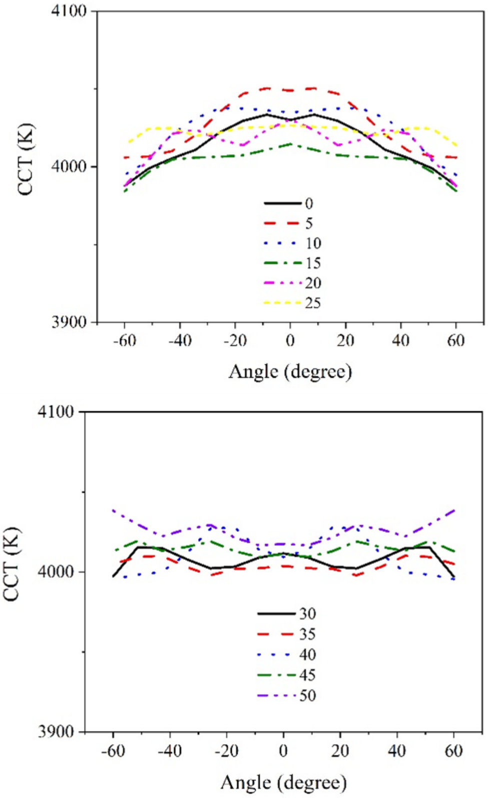

Fig. 5: The CCT range with altering the concentration of Al-doped ZnO.

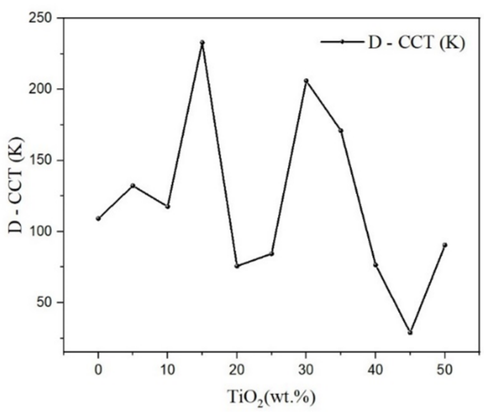

Fig. 6: The CCT delta with altering Al-doped ZnO concentration.

concentration, at 5 wt%, demonstrates sufficient scattering and conversion efficiencies, resulting in a broader color coverage on the chroma spectrum and enabling the rendered light to capture more color elements of the targeted object. However, a consistent trend emerges as Al-doped ZnO concentration exceeds 5 wt%, with a gradual reduction in both CQS and CRI parameters, even falling below the reference data (undoped sample) [26–28].

This observed trend aligns with the behavior noted in the lumen strength of the white LED. Higher concentrations of Al-doped ZnO promote the scattering of blue light and the conversion of red light, leading to a noticeable shift in the overall emission color spectrum toward the yellow-orange range. While contributing to a decline in color reproduction quality due to the reduced presence of blue light, these findings emphasize that the most favorable Al-doped ZnO concentration for both lumen output and color rendition is at 5 wt%. This concentration not only enhances color reproduction but also strikes a delicate balance between color quality and the overall luminosity of the white LED.

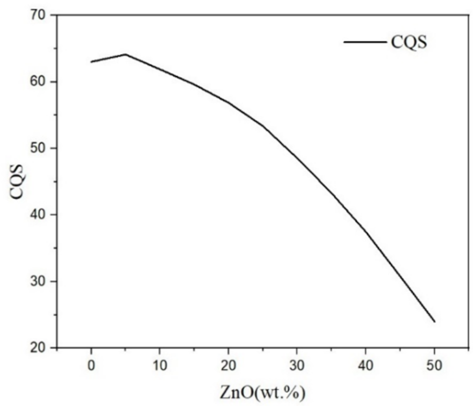

Fig. 7: CQS with altering the concentration of Al-doped ZnO.

4. Conclusions

potential of using an Al-doped ZnO film as a remote luminescent converting layer for advancing the performance of warm white LEDs. Our investigation reveals a clear correlation between the Al-doped ZnO concentration and the improvement in the scattering function, leading to a more even dispersion of colors and heightened

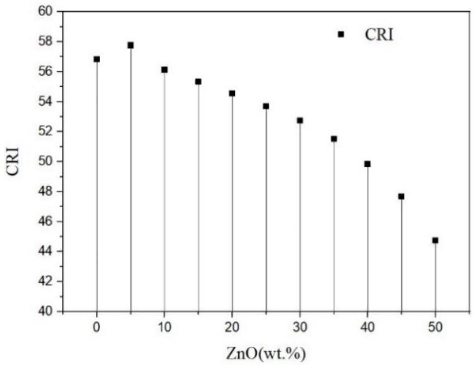

Fig. 8: CRI with altering the concentration of Al-doped ZnO.

overall color uniformity. Overall, increasing Al-doped ZnO concentration can minimize spatial color deviation for greater color uniformity of the generated white light. The lowest color deviation is obtained with the Al-doped ZnO amount of 45 wt%. Additionally, utilizing an Al- doped ZnO concentration range of 20-25 wt% demonstrates superior color uniformity compared to the undoped sample's data. Simultaneously, our study pinpoints 5 wt% Al-doped ZnO as the optimal quantity for maintaining respectable lumen strength and efficient color rendering.

However, beyond 5 wt% Al-doped ZnO, a discernible decline is observed in these parameters due to reduced luminous energy following each scattering event and a deficiency in blue-light emission, ultimately contributing to color deviation. These nuanced findings underscore the critical importance of maintaining a delicate balance in Al-doped ZnO concentration for achieving both enhanced color uniformity and satisfactory lumen output with efficient color rendition in warm white LED designs. This research not only advances our understanding of the intricate interplay between Al-doped ZnO concentration and LED performance but also provides practical insights for optimizing the design of warm white LED lighting systems for optimal efficiency and visual appeal in diverse lighting applications.

References

[1] H. D. Sang, N. T. P. Loan, H. Y. Lee, and N. D. Q. Anh. Study of K2SIF$_6$: MN4+@SIO2 phosphor for white leds with high angular color uniformity. *J. Adv. Eng. Comput.*, 8:53–62, 2024.

[2] K. F. Mendes, B. A. Maset, K. C. Mielke, R. N. De Sousa, B. A. B. Martins, and V. L. Tornisielo. Phytoremediation of quinclorac and tebuthiuron-polluted soil by green manure plants. *Int. J. Phytoremediation*, 23:474–481, 2020.

[3] N.F. Lousek, N.C. Santos, M.C.M. Dourado, F.M. Pontieri, M.N.G.Teófilo, F.S.Castro, S.H.N.Costa, G.T.Blanch, A.F.Borges, and C.M.Gomes. Effects of green banana biomass (musa spp.) on laboratory parameters of animal models of wistar mice under hyperlipidic diet. *J. Am. Coll. Nutr.*, 40:472–477, 2021.

[4] B. G. P. Leela and D. N. Rajendran. Effect of lanthanide ion co-doping on the luminescence in the cerium-doped zinc oxide-phosphor system. *Spectrosc. Lett.*, 52:431–440, 2019.

[5] X. Wang, X. Li, S. Xu, L. Cheng, J. Sun, J. Zhang, X. Zhang, and B. Chen. Luminescence properties of color-tunable YNbo4: Dy3+, Tm3+ phosphors. *J. Asian Ceram. Soc.*, 8:1066–1075, 2020.

[6] C. L. Huang, P. E. Chiang, and T. Hsu. Effect of a minute substitution on the structure and microwave dielectric properties of novel Licovo4 ceramics for ULTCC applications. *J. Asian Ceram. Soc.*, 9:1154–1164, 2021.

[7] Z. Huang, W. Chen, Q. Liu, Y. Wang, M. R. Pointer, Y. Liu, and J. Liang. Towards an optimum colour preference metric for white light sources: a comprehensive investigation based on empirical data. *Opt. Express*, 29:6302, 2021.

[8] R. Wan, X. Gao, L. Wang, S. Zhang, X. Chen, Z. Liu, X. Yi, J. Wang, J. Li, W. Zhu, and J. Li. Phosphor-free single chip

gan-based white light emitting diodes with a moderate color rendering index and significantly enhanced communications bandwidth. *Photonics Res.*, 8:1110, 2020.

[9] S. J. Dain, D. A. Atchison, J. K. Hovis, and M. Y. Boon. Lighting for color vision examination in the era of LEDs: the FM100Hue test. *J. Opt. Soc. Am. A*, 37:A122–A132, 2020.

[10] Y. Yu, C. Cao, Z. Wu, Q. Wu, W. Lin, X. Peng, Y. Jin, X. Zhang, H. Yang, and Q. Tong. Improving the color-rendering index of a tandem warm white organic light-emitting device by employing a simple fabrication process. *Opt. Lett.*, 44:931, 2019.

[11] P. Zhu, H. Zhu, G. C. Adhikari, and S. Thapa. Design of circadian white light-emitting diodes with tunable color temperature and nearly perfect color rendition. *OSA Continuum*, 2:2413, 2019.

[12] X. Hu, Y. Lian, Z. Liu, Y. Jin, Y. Hu, Y. Liu, M. Huang, and Z. Lin. Optimizing selection of the test color sample set for the CIE 2017 color fidelity index. *Opt. Express*, 28:8407, 2020.

[13] K. Huraibat, E. Perales, E. Kirchner, I. Van Der Lans, A. Ferrero, and J. Campos. Accurate physics-based digital reproduction of effect coatings. *Opt. Express*, 29:34671, 2021.

[14] S. Thapa, G. C. Adhikari, H. Zhu, A. Grigoriev, and P. Zhu. Zn-alloyed all-inorganic halide perovskite-based white light-emitting diodes with superior color quality. *Sci. Reports*, 9:18636, 2019.

[15] M. Gupta, A. K. Dubey, V. Kumar, and D. S. Mehta. Indoor daylighting using fresnel lens solar-concentrator-based hybrid cylindrical luminaire for illumination and water heating. *Appl. Opt.*, 59:5358, 2020.

[16] G. Yang, Y. Zhu, X. Li, J. Huang, X. Xu, X. Ji, A. Wang, J. Cheng, and G. Pan. Double perovskite microcrystals-based white light-emitting diodes without reabsorption of multiphase phosphors. *Opt. Lett.*, 46:6043–6046, 2021.

[17] J. Du, Y. An, D. Wu, C. Wang, C. Zhu, X. Li, and D. Ma. Easy-to-process and high-performance colorful perovskite solar cells using a multilayer planar filter. *Opt. Lett.*, 45:6326–6329, 2020.

[18] A. Eissfeldt, B. Zandi, A. G. Herzog, and T. Q. Khanh. Quantifying observer metamerism of led spectra which chromatically mimic natural daylight. *Opt. Express*, 29:38168, 2021.

[19] S. Donati, W.-H. Cheng, C.-N. Liu, H.-K. Shih, and Z. Pei. Embedding LiDAR and smart laser headlight in a compact module for autonomous driving. *OSA Continuum*, 4:1587, 2021.

[20] T. Urner, A. Inman, B. Lapid, and S. Jia. Three-dimensional light-field microendoscopy with a GRIN lens array. *Biomed. Opt. Express*, 13:590, 2022.

[21] K. Ichikawa, S. Yokoyama, Y. Tanaka, H. Nakamura, S. Rjh, and S. Tanabe. The change in color vision with normal aging evaluated on standard pseudoisochromatic plates part-3. *Curr. Eye Res.*, 46:1038–1046, 2020.

[22] F. Feltrin, F. Leccese, P. Hanselaer, and K. Smet. Impact of illumination correlated color temperature, background lightness, and painting color content on color appearance and appreciation of paintings. *Leukos*, 16:25–44, 2020.

[23] W. Mao, W. Bao, and H. P. Huang. Consideration of light level in specifying light source color rendition. *Leukos*, 16:55–65, 2018.

[24] L. A. Tuan and H. Y. Lee. A new effective K7SRY2B15O30: EU3+ sample for white leds yielding non-dosage abatement as well as strong heat consistency. *J. Adv. Eng. Comput.*, 8:63–74, 2024.

[25] J. W. Han, C. W. Joo, J. Lee, D. J. Lee, J. Kang, S. Yu, W. J. Sung, N. S. Cho, and Y. H. Kim. Enhanced out-coupling in down-conversion white organic

light-emitting diodes using imprinted microlens array films with breath figure patterns. *Sci. Technol. Adv. Mater.*, 20:35–41, 2019.

[26] N. Thong, D. Son, S. Ho, N. Q. Anh, and H. Lee. The use of Y3Al5O12:Ce3+ and CaTiO3:Pr3+ in a dual-layer remote phosphor configuration improves the optical efficiencies of a phosphor-in-glass white light-emitting diode. *J. Adv. Eng. Comput.*, 6:36–44, 2022.

[27] A. Le, S. Ho, D. Nguyen, and H. Lee. Triple-layer design of YVO4:Eu3+, YF3:Mn2+, and YAG:Ce3+: the potential for advancement of remote phosphor structure to get better chromaticity and luminescence at high color temperatures. *J. Adv. Eng. Comput.*, 6:113–121, 2022.

[28] M. Lai, H. Lee, and D. Nguyen. Exellent color quality and luminous flux of wleds using triple-layer remote phosphor configuration. *J. Adv. Eng. Comput.*, 4:74–82, 2020.

About Authors

Hsin-Yi MA was born in Hsinchu city, Taiwan. She has been working at the Department of Industrial Engineering and Management, Minghsin University of Science and Technology, Hsinchu, Taiwan. Her research interest is Production optimization and Optics.

Nguyen Doan Quoc ANH was born in Khanh Hoa province, Vietnam. He has been working at the Faculty of Electrical and Electronics Engineering, Ton Duc Thang University. Quoc Anh received his PhD degree from National Kaohsiung University of Science and Technology, Taiwan in 2014. His research interest is optoelectronics.

